American Mineralogist, Volume 80, pages 94–108, 1995

H_2O solubility in haplogranitic melts: Compositional, pressure, and temperature dependence

François Holtz

Centre de Recherches sur la Synthèse et la Chimie des Minéraux, CRSCM-CNRS, 1A rue de la Férollerie, 45071 Orléans, France

Harald Behrens

Institut für Mineralogie, University of Hanover, Welfengarten 1, 30167 Hanover, Germany

Donald B. Dingwell

Bayerisches Geoinstitut, University of Bayreuth, Postfach 10 12 51, 95440 Bayreuth, Germany

Wilhelm Johannes

Institut für Mineralogie, University of Hanover, Welfengarten 1, 30167 Hanover, Germany

Abstract

H_2O solubility has been determined in haplogranitic melts (system SiO_2-$NaAlSi_3O_8$-$KAlSi_3O_8$, Qz-Ab-Or) in the range 0.5–8 kbar and 800–1350 °C. Three types of starting materials were used: dry glass cylinders, prehydrated glass pieces, or dry glass blocks surrounded by glass powder. All the starting materials gave consistent results. The H_2O contents of the glasses were determined by Karl-Fischer titration. Dissolved H_2O was demonstrated to be distributed homogeneously throughout the isobarically quenched melts (glasses) using infrared spectroscopy.

The compositional dependence of H_2O solubility was mainly determined at 0.5 kbar, 900 and 1000 °C; 1 kbar, 850 °C; and 4.8 kbar, 800 °C. Seventeen compositions containing 25, 35, or 45 wt% normative Qz and with various Or/(Or + Ab) ratios (0.86–0.09, Ab and Or expressed as normative weight percent) were investigated. At 0.5 kbar, H_2O solubility was little affected by the anhydrous composition. By contrast, molar H_2O solubility in aluminosilicate melts was significantly dependent upon anhydrous composition between 1 and 5 kbar. The highest solubility values were obtained for the most Ab-rich melts. This alkali effect has important implications for the physical and chemical properties of granitic melts.

The effect of pressure (P) on H_2O solubility at $P \geq 3$ kbar is greater than that reported in previous studies. Between 3 and 8 kbar at 800 °C, there is a (nearly linear) positive correlation between P and H_2O solubility. The effect of temperature (T) on H_2O solubility was investigated for a composition $Qz_{28}Ab_{38}Or_{34}$ (normative weight percent) in the P-T range 0.5–8 kbar and 800–1350 °C. Water solubility ranged from retrograde (with increasing T) at $P \leq 4$ kbar through temperature independence at approximately 4.5 kbar to prograde at $P = 5$ kbar.

Calculated H_2O solubilities using the model of Burnham and Nekvasil (1986) are slightly high at 0.5 kbar and significantly low at 5 kbar, compared with the experimental data. This implies that calculated H_2O activities for haplogranitic systems using the H_2O content of the melt may be overestimated at high pressure ($P \geq 5$ kbar). Using the thermodynamic model of Silver and Stolper (1985) and assuming a proportion of molecular H_2O and OH groups close to that defined for albite melts by Silver and Stolper (1989), we found that the partial molar volume of H_2O in a melt with a composition $Qz_{28}Ab_{38}Or_{34}$ has to be close to 10–12 cm^3/mol to obtain a good agreement between the calculated and the experimentally determined H_2O solubility curves in the pressure range 1–8 kbar at 900 °C.

Introduction

H_2O influences both the physical and chemical properties of granitic magmas, and the investigation of the pressure, temperature, and composition dependence of H_2O solubility in haplogranitic melts (system SiO_2-$NaAlSi_3O_8$-$KAlSi_3O_8$, Qz-Ab-Or) has important petrological implications. The available H_2O solubility data for granitic systems have been for the most part obtained either from natural granitic compositions or from some synthetic compositions. Data from natural rocks ob-

0003–004X/95/0102–0094$02.00

tained for a single multicomponent composition cannot however be easily interpreted and extended to other compositions because certain elements (e.g., F, B, Li), although present only in low concentrations, may influence significantly the H_2O solubility in the melt (e.g., Pichavant, 1983; Sorapure and Hamilton, 1984; Holtz et al., 1993). There are few data from synthetic compositions in the system Qz-Ab-Or. In addition, there are significant variations in the data for a given pressure (P), temperature (T), and composition (for Ab melts, see reviews by Dingwell, 1987, and Behrens, in preparation) due to the use of differing experimental methods, starting materials, and analytical techniques for the determination of the H_2O content (Dingwell et al., 1984; McMillan and Holloway, 1987; Behrens, in preparation). Data obtained by different methods are not directly comparable, and the absolute value of H_2O solubility can only be stated within a relatively large uncertainty.

For these reasons, an internally consistent H_2O solubility data set for compositions in the system Qz-Ab-Or is needed to understand the effects of H_2O on the phase relations and evolution of melts in the haplogranite system and to test predictions of various solubility models. In the present study, H_2O solubility was investigated in 17 ternary Qz-Ab-Or melt compositions. The compositional dependence of H_2O solubility was investigated at 0.5, 0.52, 1, 4.8, and 5 kbar. The results are complementary to our previous work (Holtz et al., 1992a), in which the compositional dependence was investigated at 2 kbar. In both studies, the same experimental and analytical method has been used to obtain a consistent data set. The effects of P and T on H_2O solubility have been extensively investigated for one composition ($Qz_{28}Ab_{38}Or_{34}$, subscripts in weight percent).

Starting material and experimental techniques

Starting glasses

The starting materials for preparation of the haplogranite glasses were powders of Na_2CO_3, K_2CO_3, Al_2O_3, and SiO_2. Sixteen compositions (HPG1–HPG16, Table 1) with three different normative Qz contents (Qz_{45}, Qz_{35}, Qz_{25}) and different Or/(Or + Ab) ratios were synthesized. The powders of the starting materials (weighted to obtain 70–100 g of glass for each composition) were dried at 120 °C and mixed. The mixtures were fused directly at 1600 °C over a period of several hours. The products of the initial fusions were bubble-rich and heterogeneous. To remove the bubbles and promote homogenization, the fused batches were loaded into a box furnace, reheated at 1700 °C, and stirred for several days until virtually devoid of bubbles. Bubble-free melts were cooled slowly in the box furnace to <800 °C and then removed from the furnace. The glass used for the investigation of pressure and temperature dependence (composition AOQ, Table 1) was prepared by the Schott Company (Mainz, Germany; melting number N8886) and contained a few bubbles.

The homogeneity and composition of the anhydrous starting glasses were determined by electron microprobe analysis (Cameca SX50, Bayerisches Geoinstitut, Bayreuth). The results of the analyses are given in Table 1 as the proportions of the oxides and as recalculated CIPW normative contents of quartz (Qz), albite (Ab), and orthoclase (Or). The investigated compositions at 0.5, 1, and 4.8 kbar are also plotted in the Qz-Ab-Or ternary diagrams in Figures 1–3 (open circles for HPG glasses, diamond for AOQ glass).

Apparatus

Internally heated gas pressure vessels (IHPV) pressurized with Ar and cold-seal pressure vessels (CSPV) pressurized with H_2O were used to conduct the experiments between 0.5 and 5 kbar. The experiments at 0.5 and 0.52 kbar, 1000 °C; 1 kbar, 1350 °C; and 4.8 kbar, 800 °C were performed at CRSCM in Orléans (IHPV). The other experiments were carried out at the University of Hanover (CSPV at $T < 900$ °C and IHPV at $T > 900$ °C). A piston-cylinder apparatus (University of Hanover) was used for the 8-kbar experiments.

Three IHPV have been used for the experiments performed at Orléans: one working horizontally with 4 Ni-NiCr thermocouples (experiments at 1000 °C) and two working vertically with 3 Ni-NiCr thermocouples (experiments at 800 °C: Roux and Lefèvre, 1992) and 5 $PtRh_6$-$PtRh_{30}$ thermocouples (high-temperature experiment at 1350 °C: Roux et al., 1994). The IHPV used at Hanover works horizontally (Ni-NiCr thermocouples). In all the IHPV, the maximal thermal gradients in the hot-spot zones (where the samples were placed) was 10 °C. Pressure was measured with transducers calibrated against Heise-Bourdon tube gauges (error ±20 bars). All Ni-NiCr thermocouples were calibrated against NaCl, Au, or Ag melting points. The CSPV work horizontally with Ni-CrNi thermocouples placed externally and calibrated against a certified thermocouple. The vessel-furnace pairs and the temperatures in the vessel were also calibrated periodically. The actual temperatures are believed to be accurate to within ±10 °C (Puziewicz and Johannes, 1988). Pressure was measured with a strain-gauge manometer (accuracy ±20 bars).

Experimental procedure and duration

The following procedure was used for all experiments carried out to define the compositional dependence of H_2O solubility (experiments with samples HPG1–HPG16). Small anhydrous glass cylinders were drilled (diameter: 3 mm; length: 2–3 mm; weight: approximately 50 mg). In each Au capsule (diameter: 4 mm; length: approximately 15 mm), one cylinder was sealed together with doubly distilled H_2O. The amount of added H_2O was chosen to be slightly higher than the expected solubility value (5, 7, and 15 wt% H_2O were added for experiments performed at 0.5, 1, and 5 kbar, respectively). The capsules were checked for possible leakage by testing for weight loss after drying in an oven at 100–120 °C for

TABLE 1. Composition of starting glasses

No.	HPG1	HPG2	HPG3	HPG4	HPG5	HPG6	HPG7	HPG8	HPG9	HPG10	HPG11
Qz,Ab,Or	28,57,15	27,48,25	26,39,35	27,29,44	27,18,55	40,55,05	37,48,15	36,39,25	37,28,35	36,19,45	36,09,55
						Composition in wt% oxides					
K_2O	2.55	4.24	5.92	7.48	9.25	0.89	2.61	4.23	5.89	7.50	9.24
Na_2O	6.71	5.74	4.63	3.50	2.38	6.48	5.67	4.60	3.46	2.38	1.21
Al_2O_3	14.11	13.94	13.95	13.70	13.55	12.43	12.25	12.07	11.83	11.85	11.79
SiO_2	76.63	76.08	75.50	75.32	74.82	80.19	79.47	79.10	78.82	78.27	77.76
						CIPW norm (wt%)					
Qz	27.85	26.75	26.14	26.86	26.70	39.10	36.51	36.38	36.86	36.27	35.96
Or	15.07	25.00	34.93	44.30	54.61	5.26	15.42	25.00	34.80	44.32	54.60
Ab	56.70	48.15	38.85	28.78	18.25	54.83	47.97	38.53	28.06	19.20	9.20
C	0.38	—	—	—	—	0.81	0.10	—	—	—	—
KS	—	0.03	0.04	0.04	0.33	—	—	0.04	0.15	0.15	0.21
NaS	—	0.07	0.04	0.02	0.11	—	—	0.05	0.13	0.07	0.03
						Mole proportions					
Or/(Ab + Or)	0.200	0.328	0.459	0.592	0.738	0.083	0.232	0.379	0.539	0.640	0.848
						Dry molecular weight on one O basis					
	32.24	32.46	32.67	32.83	33.05	31.75	32.00	32.19	32.36	32.55	32.75

Note: compositions are average values of 10 microprobe analyses and are normalized to 100%. Glasses labeled HPG were synthesized by ourselves. Glass labeled AOQ was synthesized by Schott Company, Mainz, Germany. Qz = quartz; Ab = albite; Or = orthoclase; C = corundum; KS = K_2SiO_3; NaS = Na_2SiO_3.

at least 1 h. The investigated *P-T* conditions are given in Table 2.

Three methods were used to prepare the charges for the investigation of temperature and pressure dependence of H_2O solubility using the glass AOQ ($Qz_{28}Ab_{38}Or_{34}$). Most samples consisted of single glass blocks (dry or containing a known amount of H_2O; 22 expts. in Table 3). Other samples consisted of either a glass block surrounded by glass powder, or glass powder alone. The applied *P-T* conditions and the amount of added H_2O are given in Table 3.

The large volume of the IHPV used at Orléans allowed large numbers of capsules to react in a single experiment at nearly identical *P-T* conditions. For the results obtained at 0.5 kbar and 1000 °C, 17 capsules (corresponding to 17 compositions) reacted in a single experiment. Similarly, one experiment was performed to produce the eight 0.52-kbar glasses (at 1000 °C). The data at 4.8 kbar were obtained from two experiments (2 × 10 capsules). Thus, for the data obtained at these conditions, variations in H_2O solubilities are unlikely to be due to variations of pressure or temperature between experiments. In

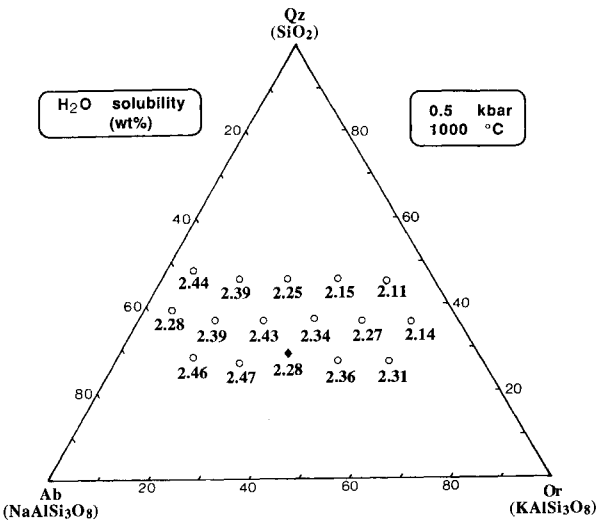

Fig. 1. H_2O solubility, expressed as wt% H_2O, for 16 melt compositions (circles and diamond) of the haplogranite system Qz-Ab-Or at 0.5 kbar and 1000 °C. The solubility value for each composition is indicated under the corresponding circle. The Qz, Ab, and Or contents of the investigated compositions are given as wt% normative proportions. All corresponding experimental conditions and analytical data are given in Tables 1–3. The diamond represents the AOQ composition ($Qz_{28}Ab_{38}Or_{34}$), for which the temperature dependence of H_2O solubility was investigated.

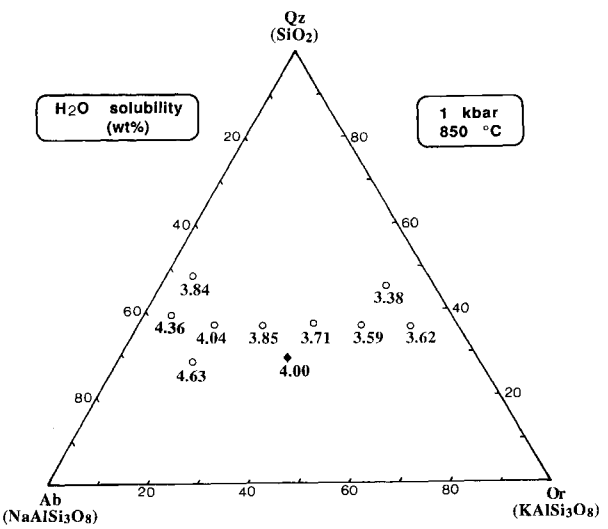

Fig. 2. H_2O solubility, expressed as wt% H_2O, for 10 melt compositions of the haplogranite system Qz-Ab-Or at 1 kbar, 850 °C. Same remarks as for Fig. 1.

TABLE 1.—*Continued*

HPG12 48,47,05	HPG13 46,39,15	HPG14 46,29,25	HPG15 46,19,35	HPG16 45,10,45	AOQ 28,38,34
		Composition in wt% oxides			
0.89	2.64	4.21	5.90	7.64	5.68
5.46	4.54	3.48	2.37	1.21	4.65
10.59	10.45	10.24	10.09	10.13	13.53
83.06	82.37	82.06	81.64	81.03	76.14
		CIPW norm (wt%)			
47.90	45.86	45.84	45.86	45.13	28.16
5.26	15.60	24.88	34.86	45.14	33.59
46.20	38.41	29.23	19.05	9.57	37.92
0.64	0.12	—	—	—	—
—	—	0.02	0.15	0.13	0.16
—	—	0.03	0.08	0.03	0.17
		Mole proportions			
0.097	0.277	0.439	0.633	0.816	0.455
		Dry molecular weight on one O basis			
31.51	31.62	31.91	32.10	32.30	32.60

contrast, only two capsules could be placed simultaneously in the CSPV. Therefore, slight variations of pressure may exist in the data obtained at 1 and 5 kbar.

The capsules were kept at the desired P and T for sufficient time to allow complete homogenization by diffusion of H_2O through the sample (more details are given in the following discussion). The experimental duration was 10–20 d for all experiments performed in order to define the compositional dependence of H_2O solubility (Table 2) and for the experiments carried out with anhydrous starting glass $Qz_{28}Ab_{38}Or_{34}$ at temperatures between 750 and 850 °C (Table 3). The durations were lower at higher T and when the starting solid material contained H_2O (2–5 d for most expts., Table 3) because diffusion of H_2O is faster at high T and in hydrous glasses.

Quenching in CSPV was performed by using a flow of

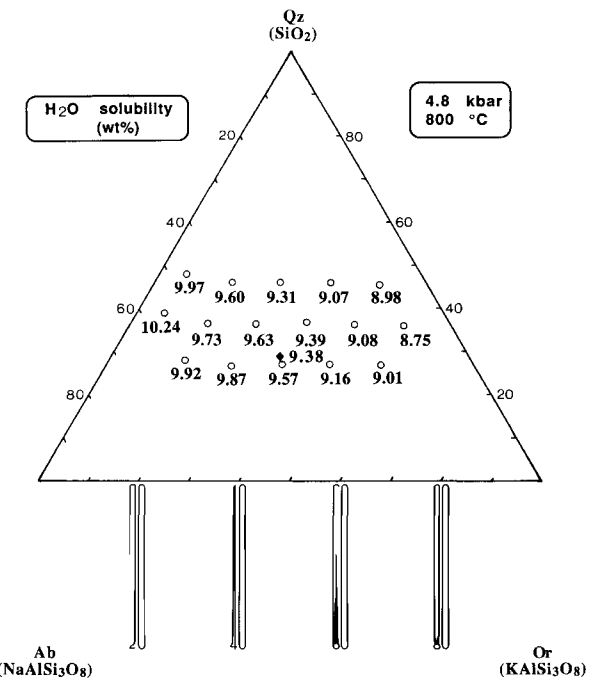

Fig. 3. H_2O solubility, expressed as wt% H_2O, for 17 melt compositions of the haplogranite system Qz-Ab-Or at 4.8 kbar and 800 °C. Same remarks as for Fig. 1.

TABLE 2. Measured H_2O contents in haplogranite glasses

Glass no.	P (kbar)	T (°C)	Trial 1 H_2O content (wt% H_2O)	Trial 1 t (d)	Trial 2 H_2O content (wt% H_2O)	Trial 2 t (d)	Trial 3 H_2O content (wt% H_2O)	Trial 3 t (d)	H_2O solubility (wt%)
HPG1	0.5*	1000	2.36	12					2.46
	1	850	4.50	11	4.57	14			4.63
	4.8*	800	9.80	21	9.85	15			9.92
HPG2	0.5*	1000	2.37	12					2.47
	4.8*	800	9.77	15					9.87
HPG3	5	800	9.53	12					9.63
	4.8*	800	9.47	15					9.57
HPG4	0.5*	1000	2.26	12					2.36
	4.8*	800	9.06	15					9.16
HPG5	0.5*	1000	2.21	12					2.31
	4.8*	800	8.91	21					9.01
	5	800	9.44	11					9.54
HPG6	0.5	900	2.56	10	2.44	14	2.31	11	2.54
	0.5*	1000	2.18	12					2.28
	0.52*	1000	2.49	17					2.59
	1	850	4.18	12	4.34	10			4.36
	4.8*	800	10.23	21	10.05	15			10.24
	5	800	10.37	11					10.47
HPG7	0.5	800	2.55	12					2.65
	0.5	900	2.51	12**					2.59
			2.47	12**					
	0.5*	1000	2.29	12					2.39
	0.52*	1000	2.57	17**					2.68
			2.60	17**					
	1	850	4.10	12	3.92	10	3.80	14	4.04
	4.8*	800	9.63	21					9.73
HPG8	0.5	850	2.55	12					2.65
	0.5*	1000	2.33	12					2.43
	0.52*	1000	2.45	17**					2.50
			2.35	17**					
	1	850	3.69	12	3.81	10			3.85
	4.8*	800	9.53	21					9.63
	5	800	9.90	11					10.00
HPG9	0.5*	1000	2.24	12					2.34
	0.52*	1000	2.34	17					2.44
	1	850	3.52	12	3.70	14			3.71
	4.8*	800	9.29	21					9.39
	5	800	9.80	13					9.90
HPG10	0.5	900	2.23	12	2.26	14	2.46	11	2.42
	0.5*	1000	2.17	12					2.27
	0.52*	1000	2.27	17					2.37
	1	850	3.75	12	3.46	10	3.27	16	3.59
	4.8*	800	8.98	21					9.08
	5	800	9.01	13					9.11
HPG11	0.5	900	2.21	12	2.14	14			2.27
	0.5*	1000	2.04	12					2.14
	0.52*	1000	2.20	17					2.30
	1	850	3.41	10	3.64	16			3.62
	4.8*	800	8.72	21	8.59	15			8.75
HPG12	0.5*	1000	2.34	12					2.44
	0.52*	1000	2.42	17					2.52
	1	850	3.57	12	3.65	14	4.01	11	3.84
	4.8*	800	9.87	21					9.97
	5	800	9.65	10					9.75
HPG13	0.5*	1000	2.29	12					2.39
	4.8*	800	9.50	15					9.60
HPG14	0.5*	1000	2.15	12					2.25
	4.8*	800	9.21	15					9.31
HPG15	0.5*	1000	2.05	12					2.15
	0.52*	1000	2.17	17					2.27
	4.8*	800	8.97	15					9.07
HPG16	0.5*	1000	2.01	12					2.11
	1	850	3.19	12	3.38	14			3.38
	4.8*	800	8.97	21	8.79	15			8.98
	5	800	9.32	10					9.42

Note: all experiments were performed with a dry glass block as starting material. All H_2O contents are determined by KFT. For calculation of H_2O solubilities, 0.1 wt% H_2O was added to the average values (see text).

* Experiments performed in internally heated pressure vessels; all other experiments performed in cold-seal pressure vessels.

** Measurement by KFT was duplicated.

TABLE 3. Measured H_2O contents for composition AOQ ($Qz_{28}Ab_{38}Or_{34}$)

Exp.	P (kbar)	T (°C)	Starting material	Wt% H_2O added	t (h)	H_2O content of glass (wt% H_2O)	Remarks	H_2O solubility (wt%)
1	0.3	800	bp	4.2	576	2.03, 2.03		2.13
2	0.5	800	b	5.1	528	2.68, 2.70		
3	0.5	800	bp	2.9	336	2.56, 2.64, [2.72]	ib	2.80
4	0.5	800	bp	6.3	528	2.86, 2.76		
5	0.5	900	b	5.2	1056	2.78, [2.56]	ib	
6	0.5	900	b (2% H_2O)	3.1	1056	2.35, [2.50]		2.60
7	0.5	1000	b	4.0	110	2.18		2.28
8	0.5	1100	b (1% H_2O)	8.6	72	2.49, [2.29]		2.44
9	0.5	1200	b (1% H_2O)	6.5	96	2.22	ib	2.32
10	0.7	800	bp	5.4	336	3.67, 3.69, [3.75]	ib	
11	0.7	800	bp	5.4	336	3.99, [3.38]		3.75
12*	1	800	bp	5.0	240	4.20, 3.96, 3.93, 3.84, 4.12		
13*	1	800	bp	6.0	504	4.05**, 4.20†		
						[3.94‡, 3.92‡, 3.96‡, 4.05†, 4.08†, 4.14†]		4.09
14*	1	800	bp	6.0	504	4.11**, 4.05†	ib	
						[4.04‡, 4.13‡, 4.09‡, 4.09†, 4.12†, 3.93†]		
35	1	1200	b (3% H_2O)	7.7	70	3.53, [3.46]	ib	3.54
36	1	1350	b	7.0	121	[3.38]		3.38
15	1	850	b	6.5	816	3.85, 3.96		4.00
16	1.3	800	bp	5.1	336	5.07, 4.90, 4.95, [4.87]	ib	5.02
17	1.4	800	p	7.1	480	5.14, [5.08]	ib	5.16
18	3	800	b	10.9	264	7.35		
19	3	800	b	11.1	508	7.24, 7.46		7.45
20	3	1200	b	15.0	704	7.15		7.25
21*	4	800	bp	10.4	336	8.66‡, 8.84‡, 8.93†, 8.94†		8.94
37	4	1200	b (6% H_2O)	15.2	70	8.63	qb	8.73
22	4.8	800	b	15.0	502	9.28	qb	9.38
23	5	700	bp	13.0	480	9.90, 10.04	qb	10.07
24	5	800	b (5.5% H_2O)	8.2	120	9.89, 9.71	qb	
25	5	800	b (5.5% H_2O)	7.6	672	9.97		
26*	5	800	bp	11.5	240	9.71‡, 9.88‡, 9.76‡, 9.70‡		
27a	5	800	bp	13.1	768	9.92	qb	9.97
27b	5	800	b (9.9% H_2O)	3.0	16	9.94	s,qb	
27c	5	800	b (9.9% H_2O)	3.0	16	9.84	r	
28	5	850	b	14.5	60	10.38	qb	10.48
29	5	1000	b (5.5% H_2O)	8.0	96	10.56, 10.54	qb	10.65
30	5	1100	b	20.3	100	10.84	qb	
31	5	1100	b (6% H_2O)	9.0	70	10.59	qb	10.81
32	5	1200	b (6% H_2O)	19.8	48	10.75	qb	10.85
33	8	800	b (5.5% H_2O)	16.2	96	13.85, 13.32§	qb	
34	8	800	b (5.5% H_2O)	12.3	96	13.58, 13.62	qb	13.82

Note: H_2O contents were determined by KFT except for values indicated in brackets, which were determined by IR spectroscopy. In the case of several experimental products, the determination of the H_2O content was repeated: all values that were obtained are given in the table. The given H_2O solubilities are average values of the H_2O contents determined. For calculation of the average value, 0.1 wt% H_2O was added to all H_2O contents determined by KFT (see text). Symbols are defined as b = starting material was a glass block—hydrous blocks have weight percent H_2O given in parentheses; p = starting material was powder of anhydrous glass; bp = starting material was an anhydrous glass block surrounded by anhydrous glass powder; ib = the experimental product contained inclusion bubbles; qb = the experimental glass contained quench bubbles; s = slow quench rate; r = rapid quench rate.

* Large samples (up to 15 mm). KFT was performed on slices of glass cut orthogonally to the elongation of the hydrous glass cylinder.

** H_2O solubility was determined in a part of the glass corresponding to both powdered starting material and glass block.

† H_2O solubility was determined in a part of the glass corresponding to the starting glass block.

‡ H_2O solubility was determined in a part of the glass corresponding to the starting powdered material.

§ The H_2O content is not used to calculate the H_2O solubility (see explanation in text).

compressed air. Quenching in IHPV was obtained by switching off the heating power. Isobaric quenching was performed for all experiments, except the two experiments at 4.8 kbar and 800 °C. In the case of these two experiments, the temperature dropped from 800 to 350 °C in <4 min, and pressure dropped from 4.8 to 3.2 kbar.

ANALYTICAL TECHNIQUES

Karl Fischer titration (KFT)

The H_2O content of the quenched glasses was determined by Karl Fischer titration (Turek et al., 1976; Westrich, 1987; Holtz et al., 1992a; Behrens, in preparation). In this procedure, the hydrous glasses, placed in a Pt crucible, are heated progressively from 20 to 1300 °C using an induction furnace. The liberated H_2O is transported by a dry Ar stream to the titration cell. The analytical method (KFT) was calibrated using standards with known H_2O contents, such as calcium sulfate dihydrate, sodium tartrate dihydrate, muscovite, and hydrous glasses. The measured H_2O contents were in good agreement with the expected values (Behrens, in preparation).

Only small amounts of glass are necessary to get reliable data (typically 10–20 mg of substances containing about 6 wt% H_2O were used). Single pieces or roughly

crushed glass were used rather than finely powdered glass in order to minimize possible errors due to absorption of H_2O (for glasses with low H_2O contents) or to desorption (for glasses with high H_2O contents). For glasses with high H_2O contents (>6 wt%) a block of hydrous glass was placed directly in the Pt crucible. For glasses with low H_2O contents (<6 wt% H_2O), roughly crushed glass was preferred to single pieces for the measurements because sputtering of the glass can occur by explosive liberation of H_2O. The H_2O content was determined quickly after crushing. Holtz et al. (1992a) have checked that the H_2O contents measured using either a single piece of hydrous glass or a freshly crushed powder of the same material were identical within error (Table 3 in Holtz et al., 1992a).

The analytical precision for H_2O is mainly dependent on the duration of the titration and on the amount of sample. The weight of the analyzed samples has usually been chosen so that the amount of measured H_2O is 500–1500 μg. The duration of the titration was 7–10 min. With these analytical conditions, the precision is less than or equal to ± 0.15 wt% H_2O. Duplicate analyses gave results within the analytical precision given above (see Table 2, compositions HPG7 and HPG8; Table 3, expt. nos. 2, 15, 19, 24, 29, and 34, with AOQ starting materials composed of glass blocks only), except for one experiment at 8 kbar (Table 3, no. 33), which is discussed later. The relative variation of H_2O contents from these duplicate analyses is always <4%. Variations lower than 1% relative were also systematically found for 10 experimental products obtained at 2 kbar for composition AOQ (see analytical data in Tables 2 and 3 in Holtz et al., 1992a). The largest variations obtained by duplicating the analyses (0.1–0.2 wt% H_2O) can be explained by sputtering of the glass during the heating period of KFT caused by explosive liberation of H_2O. This can lower artificially the measured H_2O content of the glass because small pieces of hydrous glass may fall out of the hot zone of the induction furnace.

Other analytical techniques

The H_2O solubility was also determined by the weight-loss method (punctured capsule placed at 105 °C for 1 h) for some samples. For low H_2O contents (<7 wt% H_2O), the results obtained by KFT and weight loss are in good agreement. For example, H_2O contents of AOQ glasses synthesized at 0.5 and 2 kbar were found to be 2.69, 2.81, 5.10, 5.31, and 5.80 by KFT and 2.4, 2.6, 5.1, 5.2, and 5.9 by weight loss, respectively. However, for higher H_2O contents (>7 wt% H_2O), significant amounts of H_2O can diffuse from the glass heated at 105 °C, and the weight-loss method artificially decreases the measured H_2O contents. For example, after heating the glass at 105 °C for 0.5 h, >1.6 wt% H_2O was released from an albite glass that was saturated with respect to H_2O at 5 kbar and 1100 °C and contained initially 11.8 wt% H_2O (data given in Behrens, 1995).

Infrared microspectroscopy (Bruker IFS 88 and microscope A590 at Hanover, Nicolet FTIR 710 and the microscope Nicplan at Orléans) has been used to measure the homogeneity of the hydrous glasses. The microanalytical method allows local resolution of 100–50 μm. The H_2O contents of AOQ glass samples have been determined by measuring the height at the maximum of the absorption bands near 4500 and 5200 cm^{-1}, assigned to OH groups and molecular H_2O, respectively (Stolper, 1982). Linear molar absorptivities were determined to be 1.60 ± 0.03 L/mol·cm (OH groups) and 1.79 ± 0.02 L/mol·cm (molecular H_2O) by using reference samples analyzed by KFT. Using these standards, the density (in g/L) of the glasses is given by: $\rho_{(g/L)} = 2347 - 12.6 \cdot C(H_2O)$ (wt%). The results obtained by infrared spectroscopy are given in brackets in Table 3.

Results: H_2O content of quenched haplogranite glasses and H_2O solubility

The H_2O contents of all analyzed glasses are given in Table 2 (HPG samples) and Table 3 (AOQ). For most experiments at $P < 4.8$ kbar with a starting glass composed of a block only, the quenched products consisted of bubble and crystal-free clear glasses. In several experiments at $P \geq 4.8$ kbar, Or-rich glasses show homogeneously distributed bubbles (the glass is cloudy) of almost uniform size, which are attributed to an oversaturation of bubble and crystal-free clear glasses. In several experiments at $P \geq 4.8$ kbar, Or-rich glasses show homogeneously distributed bubbles (the glass is cloudy) of almost $P \leq 1.4$ kbar, the bubbles were distributed heterogeneously in the sample and showed a large variation in size. These bubbles were probably incorporated in the melt at the beginning of the experiment (inclusion bubbles).

Reproducibility of the experiments

The reproducibility of our solubility experiments was tested for different compositions, P-T conditions, and experimental apparatus. These tests were particularly important for the experiments performed with CSPV (only two capsules could be placed simultaneously in the vessel) and for the experiments carried out to define the temperature and pressure dependence of H_2O solubility (a small deviation of the pressure may affect significantly the H_2O solubility). The results given in Tables 2 and 3 show that little variation in H_2O content is observed when comparing data obtained from different experiments at the same P-T conditions. The maximal relative variation is 10% at 0.5 kbar (absolute variation: 0.25 wt% H_2O; Table 2, HPG6, HPG10, and HPG11; Table 3, nos. 2, 3, and 4) and 7% at 1 kbar (except two experiments with 12.8 and 13% relative variation; Table 2, HPG1, HPG6–HPG12). The relative variations are lower for higher pressures (Table 3) and are <2% for the experiments at 4.8 kbar and 800 °C (Table 2, HPG1, HPG11, and HPG16). In addition, the glasses from the experiment performed at 0.52 kbar and 1000 °C show systematically slightly higher H_2O contents than those obtained from the 0.5-kbar experiment (as expected from the positive dependence of H_2O solubility on P).

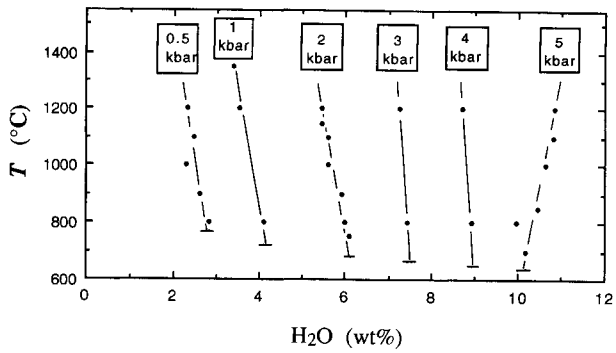

Fig. 4. Temperature dependence of H_2O solubility at 0.5, 2, 3, and 5 kbar for AOQ melt ($Qz_{28}Ab_{38}Or_{34}$). The vertical bar represents the liquidus temperature for composition AOQ (from Tuttle and Bowen, 1958; Holtz et al., 1992b). Analytical data (represented by the dots) are given in Table 3.

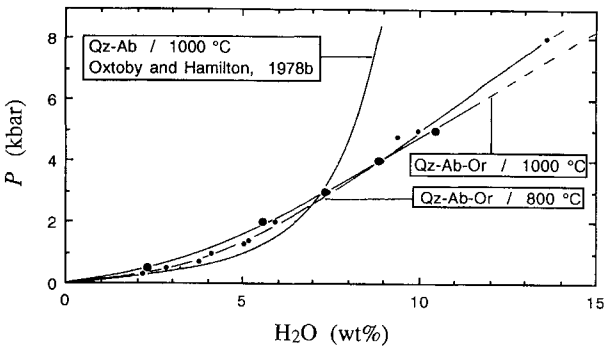

Fig. 5. Pressure dependence of H_2O solubility at 800 and 1000 °C (small dots and large dots, respectively) for AOQ melt ($Qz_{28}Ab_{38}Or_{34}$). Analytical data (represented by the dots) are given in Table 3. For comparison, data of Oxtoby and Hamilton (1978b) obtained for a Qz-Ab melt composition have been reported.

The data given in Table 3 show that the H_2O contents of glasses obtained at the same *P-T* conditions from different starting materials (dry glass block, hydrous glass block, glass block + powder) do not differ significantly. Some samples with starting materials composed of a glass block + powder were used to synthesize large amounts of hydrous glass (Table 3, nos. 12, 13, 14, 21, and 26). Profiles of the H_2O content (by KFT or infrared) along the five voluminous samples (>200 mg instead of 30–50 mg for other expts.) have been done. Three of them show that H_2O is distributed homogeneously through the samples (nos. 14, 21, and 26) whereas two of them (nos. 12 and 13) show slight variations possibly related to the starting material (powder or block in expt. 13) or to incomplete diffusion of H_2O (expt. 12; see discussion later). However, these variations remain within the analytical precision (±0.15 wt% H_2O).

Determination of H_2O solubility

There is overall very good agreement among H_2O contents determined by weight loss (for low H_2O contents), infrared spectroscopy, and KFT. However, the analysis by infrared spectroscopy of AOQ and Ab glasses after KFT showed that the residual glasses are not completely devoid of H_2O. H_2O contents of 0.10 ± 0.05 wt% H_2O were systematically found in glasses after KFT, independent of the initial H_2O content and of the composition. Thus, the H_2O contents determined by KFT have to be slightly corrected to define the H_2O solubility. This correction is also applicable to the H_2O solubility data published by Holtz et al. (1992a, 1993). In this study, the H_2O solubilities given in Tables 2 and 3 and reported in Figures 1–3 were corrected by adding 0.10 wt% H_2O to all analyses obtained by KFT (note that this also decreases slightly the analytical precision for KFT). The reported H_2O solubility for each *P-T* condition and composition (Tables 2 and 3) is the average of all analyses for that condition.

Temperature dependence of the H_2O solubility for composition $Qz_{28}Ab_{38}Or_{34}$

The temperature dependence of H_2O solubility was investigated for composition AOQ at 0.5, 1, 2, 3, 4, and 5 kbar (Table 3 and Fig. 4; 2 kbar data from Holtz et al., 1992a). There is a negative correlation between H_2O solubility and temperature at $P \leq 4$ kbar. In contrast, H_2O solubility increases with increasing *T* at 5 kbar. H_2O solubility changes by -1.6×10^{-3} wt% H_2O per degrees Celsius at 0.5, 1, and 2 kbar, by -4×10^{-4} wt% H_2O per degrees Celsius at 3 and 4 kbar, and by $+2.6 \times 10^{-3}$ wt% H_2O per degrees Celsius at 5 kbar. At 5 kbar, there may be a nonlinear variation at low *T* (800–1000 °C). However, the precision on the H_2O solubility values keeps this observation from being clearly confirmed.

The results obtained for composition AOQ at 0.5 kbar are confirmed by the results for compositions HPG6, HPG7, HPG8, HPG10, and HPG11 (Table 2). The decrease in H_2O solubility with temperature ranges between -1.3×10^{-3} wt% H_2O per degrees Celsius and -2.6×10^{-3} wt% H_2O per degrees Celsius for the five compositions, and an average value of -1.7×10^{-3} wt% H_2O per degrees Celsius is obtained.

Pressure dependence of the H_2O solubility

The effect of pressure on H_2O solubility was extensively investigated between 0.5 and 8 kbar for composition AOQ at 800 °C (Fig. 5). The H_2O solubility increase is greatest at low *P* (*P* < 1 kbar). However, the H_2O solubility increase is also significant at high *P* and is linear (+1.27 wt% H_2O per kilobar) in the pressure range 3–8 kbar. The consequence of the temperature dependence of H_2O solubility is that the effect of pressure on the H_2O solubility increase is greater at 1000 and 1200 °C than at 800 °C in the pressure range 3–5 kbar (+1.65 wt% H_2O per kilobar at 1000 °C, +1.80 wt% H_2O per kilobar at 1200 °C).

TABLE 4. H_2O solubility in wt% H_2O and mol% H_2O for haplogranite glasses at 900 °C, compared with calculated data from Burnham and Nekvasil (1986)

Glass no. Qz,Ab,Or	H_2O solubility	0.5 kbar*	1 kbar**	2 kbar†	5 kbar‡	Glass no. Qz,Ab,Or	H_2O solubility	0.5 kbar*	1 kbar**	2 kbar†	5 kbar‡
HPG1	$wt\%_{exp}$	2.62	4.55	6.26	10.43		$wt\%_{calc}$	2.73	3.97	5.66	8.48
28,57,15	$mol\%_{exp}$	(4.60)	(7.87)	(10.67)	(17.26)	HPG10	$wt\%_{exp}$	2.43	3.51	5.50	9.59
	$wt\%_{calc}$	2.83	4.09	5.88	8.77	36,19,45	$mol\%_{exp}$	(4.31)	(6.17)	(9.52)	(16.10)
HPG2	$wt\%_{exp}$	2.63	n.d.	6.08	10.38		$wt\%_{calc}$	2.72	3.95	5.63	8.44
27,48,25	$mol\%_{exp}$	(4.65)		(10.44)	(17.28)	HPG11	$wt\%_{exp}$	2.30	3.54	5.44	9.26
	$wt\%_{calc}$	2.82		5.87	8.80	36,09,55	$mol\%_{exp}$	(4.11)	(6.26)	(9.47)	(15.67)
HPG3	$wt\%_{exp}$	n.d.	n.d.	5.91	10.08		$wt\%_{calc}$	2.71	3.93	5.60	8.40
26,39,35	$mol\%_{exp}$			(10.23)	(16.87)	HPG12	$wt\%_{exp}$	2.60	3.76	6.04	10.48
	$wt\%_{calc}$			5.84	8.77	48,47,05	$mol\%_{exp}$	(4.47)	(6.40)	(10.11)	(17.01)
HPG4	$wt\%_{exp}$	2.52	n.d.	5.59	9.67		$wt\%_{calc}$	2.72	3.92	5.56	8.32
27,29,44	$mol\%_{exp}$	(4.50)		(9.74)	(16.34)	HPG13	$wt\%_{exp}$	2.55	n.d.	5.84	10.11
	$wt\%_{calc}$	2.79		5.80	8.70	46,39,15	$mol\%_{exp}$	(4.40)		(9.82)	(16.50)
HPG5	$wt\%_{exp}$	2.47	n.d.	5.33	9.52		$wt\%_{calc}$	2.71		5.57	8.33
27,18,55	$mol\%_{exp}$	(4.45)		(9.37)	(16.18)	HPG14	$wt\%_{exp}$	2.41	n.d.	5.51	9.82
	$wt\%_{calc}$	2.77		5.76	8.64	46,29,25	$mol\%_{exp}$	(4.20)		(9.37)	(16.19)
HPG6	$wt\%_{exp}$	2.44	4.28	6.43	10.75		$wt\%_{calc}$	2.70		5.54	8.29
40,55,05	$mol\%_{exp}$	(4.23)	(7.31)	(10.81)	(17.53)	HPG15	$wt\%_{exp}$	2.31	n.d.	5.57	9.58
	$wt\%_{calc}$	2.77	4.01	5.72	8.56	46,19,35	$mol\%_{exp}$	(4.05)		(9.51)	(15.89)
HPG7	$wt\%_{exp}$	2.55	3.96	6.25	10.24		$wt\%_{calc}$	2.68		5.50	8.23
37,48,15	$mol\%_{exp}$	(4.45)	(6.83)	(10.59)	(16.87)	HPG16	$wt\%_{exp}$	2.27	3.30	5.39	9.49
	$wt\%_{calc}$	2.77	4.02	5.73	8.59	45,10,45	$mol\%_{exp}$	(4.01)	(5.77)	(9.27)	(15.83)
HPG8	$wt\%_{exp}$	2.59	3.77	5.88	10.14		$wt\%_{calc}$	2.67	3.86	5.48	8.20
36,39,25	$mol\%_{exp}$	(4.54)	(6.54)	(10.04)	(16.79)	AOQ§	$wt\%_{exp}$	2.44	3.92	5.77	10.35
	$wt\%_{calc}$	2.76	4.00	5.70	8.54	28,38,34	$mol\%_{exp}$	(4.35)	(6.89)	(9.99)	(17.29)
HPG9	$wt\%_{exp}$	2.50	3.63	5.81	9.90		$wt\%_{calc}$	2.79	4.06	5.81	8.72
37,28,35	$mol\%_{exp}$	(4.41)	(6.34)	(9.98)	(16.50)						

Note: $wt\%_{exp}$ = H_2O solubility expressed as wt% H_2O, obtained from the experimental data of this study and Holtz et al. (1992a); $mol\%_{exp}$ = H_2O solubilities expressed as mol% H_2O (molecular weight of silicate is calculated on the basis of one O), obtained from the experimental data of this study and Holtz et al. (1992a); $wt\%_{calc}$ = H_2O solubility calculated using the model of Burnham and Nekvasil (1986). Following values of "ln k" were taken for the calculations: 0.5 kbar, ln k = 2.3259; 1 kbar, ln k = 1.8130; 2 kbar, ln k = 1.3836; 5 kbar, ln k = 0.9217; n.d. = not determined experimentally at the corresponding pressure.

* Using the data obtained at 1000 °C (see Table 2) and considering that H_2O solubility increases from 0.16 wt% H_2O with decreasing temperature from 1000 to 900 °C.

** Using the data obtained at 850 °C (Table 2) and considering that H_2O solubility decreases from 0.08 wt% H_2O with increasing temperature from 850 to 900 °C

† Using the data of Holtz et al. (1992a) obtained at 800 °C and considering that H_2O solubility decreases by 0.16 wt% H_2O with a temperature increase of 100 °C (H_2O solubilities are corrected by adding 0.10 wt% H_2O to the data of Holtz et al., 1992a, for explanation see text).

‡ Using the data obtained at 4.8 kbar (see Table 2) and applying a pressure correction of 1.27 wt% H_2O per kilobar and a temperature correction of 0.26 wt% H_2O with increasing temperature from 800 to 900 °C.

§ For AOQ glass, data are taken from Table 3 and Holtz et al. (1992a).

The effect of pressure on H_2O solubility observed for composition AOQ is confirmed by the data obtained with the HPG compositions (see Table 2). Although these data were not obtained for a single temperature at all pressures, the investigated temperature dependence for composition AOQ can be applied to recalculate the H_2O solubilities to 900 °C for all compositions (Table 4). The pressure dependence of H_2O solubility recalculated at 900 °C for compositions HPG11, HPG8, and HPG6 is shown in Figure 6 (HPG11, HPG8, and HPG6 are compositions with the lowest, intermediate, and the highest H_2O solubilities, respectively, for a given Qz content). The evolution of the H_2O solubility curves is similar to that of composition AOQ (Fig. 5).

Composition dependence of the H_2O solubility

The H_2O solubilities obtained at 0.5 kbar and 1000 °C (one expt.), 1 kbar and 850 °C (several expts.), and 4.8 kbar and 800 °C (two expts.) are plotted in Figures 1, 2, and 3, respectively.

At 0.5 kbar and 1000 °C, the difference between the highest and the lowest H_2O solubility is 0.36 wt% H_2O (Fig. 1). With an uncertainty of ±0.15 wt% H_2O on H_2O solubility, this result suggests that H_2O solubility is almost independent of composition at 0.5 kbar. However, the highest H_2O solubilities (>2.40 wt% H_2O) were all obtained for Ab-rich compositions and the lowest (<2.20 wt% H_2O) for Or-rich compositions. The data shown on Figure 1 suggest that, along the section HPG6–HPG11 (compositions with 35% normative Qz), a maximum H_2O solubility is attained for an intermediate composition (HPG8 with X_{Or} = 0.38). The H_2O solubilities at 900 °C (Table 2) show the same compositional dependence as at 1000 °C, although they are systematically higher (H_2O solubility at 900 °C for compositions HPG6, HPG7, HPG10, and HPG11 is 2.54, 2.59, 2.42, and 2.27 wt% H_2O, respectively), with a maximum at X_{Or} = 0.23 (composition HPG7). A maximum was also found for composition HPG7 at 0.52 kbar (H_2O solubilities are 2.59, 2.68, 2.50, 2.44, 2.37, and 2.30 wt% H_2O for compositions HPG6–HPG11, respectively). Therefore, the reproducibility of the results at three slightly different condi-

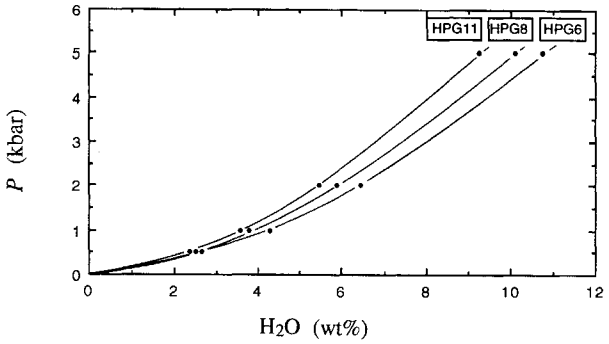

Fig. 6. Pressure dependence of H_2O solubility for melt compositions HPG6, HPG8, and HPG11. The H_2O solubility data used in this figure were recalculated for a temperature of 900 °C (for corrections applied to the experimental data, see Table 4). The normative Ab content of the melt decreased from 55 wt% for HPG6 to 9 wt% for HPG11, the normative Qz content was approximately constant (35 wt% Qz, see Table 1).

tions suggests that the maximum observed for X_{Or} between 0.23 and 0.38 is not an artifact. An effect of the Qz content of the melt on the H_2O solubility cannot clearly be demonstrated in Figure 1.

At 1 and 4.8 kbar, the highest H_2O solubilities were again obtained for Ab-rich compositions (Table 2, Figs. 2, 3, and 6) and the lowest for Or-rich compositions. At both pressures, the H_2O solubility variations were more pronounced in Ab-rich melts than in Or-rich ones. The difference in H_2O solubility between Ab- and Or-rich melts was more pronounced for compositions with low Qz contents. The effect of changing Qz content can be determined by comparing compositions with a constant Ab-Or ratio. At 1 and 4.8 kbar, the H_2O solubility increases with decreasing Qz content. This effect was more pronounced at 1 kbar than at 4.8 kbar. A relative variation of the H_2O solubility of at least 17.5% was observed at 1 kbar for compositions with approximately Or/(Ab + Or) (wt%) of 0.2, whereas it is <3.5% at 4.8 kbar. Finally, the H_2O solubility remained almost constant for a given Ab content of the melt at 4.8 kbar (Fig. 3).

The effect of the Or/(Ab + Or) molar ratio on the H_2O solubility expressed in mole percent (the molecular weight of the silicate is calculated on the basis of one O) at 900 °C is represented for compositions with 35 wt% normative Qz (HPG6–HPG11) in Figure 7. Because of the small variation of the molecular weights of the compositions (see Table 1), the same observations as stated above (from H_2O solubility in wt% H_2O) can be made. Figure 7 also shows that the compositional dependence of H_2O solubility is larger at high pressure than at low pressure, if absolute variations are considered. However, the relative variation of H_2O solubility decreased with increasing pressure from 1 to 5 kbar.

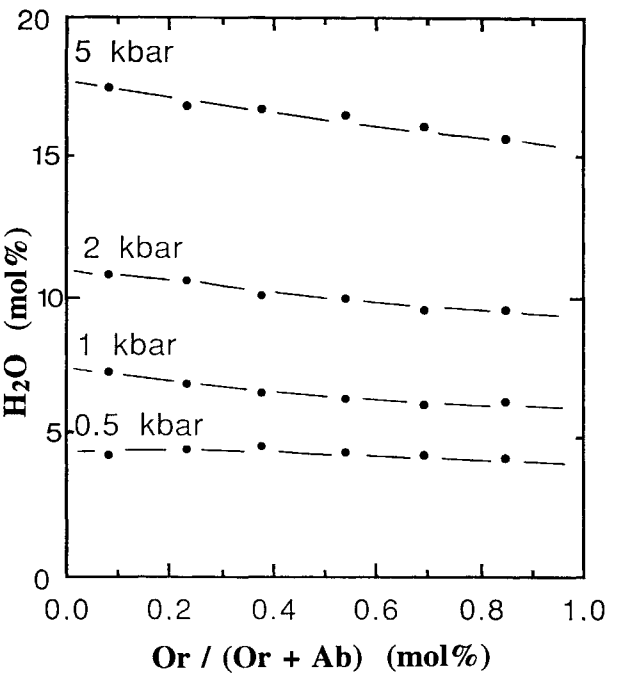

Fig. 7. Evolution of the H_2O solubility (expressed as mole percent, molecular weight of dry silicate calculated on one O basis) as a function of the Or/(Or + Ab) ratio (in mole percent) for compositions with approximately 35 wt% normative Qz (compositions HPG6–HPG11). The H_2O solubility data used in this figure are recalculated for a temperature of 900 °C (for corrections applied to the experimental data, see Table 4).

Discussion

Attainment of equilibrium

With dry or H_2O-undersaturated glass and H_2O as starting material, the reaction occurring during the experiments corresponded to a diffusion process of H_2O through the glass or liquid. Thus, at superliquidus conditions, equilibrium was attained only if H_2O was distributed homogeneously in the quenched glass and if the melt was saturated with respect to H_2O. Several observations, such as the presence of free H_2O in the capsule after quenching, confirmed visually and by the weight-loss method, showed that the melts were saturated with respect to H_2O.

The homogeneity of H_2O distribution in the glasses of the present study was tested in two ways. Some large glass samples (7–15 mm in length; 3 mm in diameter) were cut in slices of about 1-mm thickness, perpendicular to the capsule elongation. Each slice was analyzed individually by KFT. The H_2O contents obtained for three experiments at 800 °C and at 1, 4, and 5 kbar (expts. 12, 21, and 26 in Table 3) show maximal variations in H_2O content of 0.27, 0.28, and 0.17 wt% H_2O, respectively (relative variation of 8.6% at 1 kbar and <4% at 4 and 5 kbar). For the experiment at 1 kbar, it has to be noted that the highest H_2O contents (4.12 and 4.20 wt% H_2O) were found at the ends of the glass cylinder, and it may be possible that the experimental duration was too short for complete homogenization by diffusion of H_2O throughout the glass sample (15 mm in length).

Two other samples, initially consisting of single glass pieces as well as glass block plus powder, were analyzed by infrared spectroscopy (expts. 13 and 14, Table 3). The

measurements were made along a section of the cylindrical samples (local resolution of 100 μm approximately; for typical spectra obtained with glass AOQ, see Fig. 8 in Holtz et al., 1993). There was very little variation of the H_2O content in experiment 14. The H_2O contents in experiment 13 were slightly lower in the hydrous glass, which was initially powdered, when compared with the part that corresponded to the dry glass block. However, the H_2O contents were within the analytical precision. There was no difference between experiments 13 and 14, except the size of the initial powder (<200 μm in no. 14; 200–500 μm in no. 13). This suggests that small variations of H_2O contents may result from the nature of the starting material (see also Behrens, in preparation). However, except in experiment 13, all other glasses obtained with single blocks and blocks + powder (at the same P-T conditions) yielded similar H_2O contents (compare expts. 2, 3, 4 and 24, 25, 26, 27a in Table 3).

In addition to the direct evidence for homogeneous distribution of H_2O in the sample, time-dependent experiments were performed with composition AOQ. The results from experiment 12 (Table 3) suggest that 240 h were not sufficient for complete homogenization of H_2O in a sample 15 mm long at 1 kbar and 800 °C. A good homogeneity was attained in large samples obtained at 5 kbar and 800 °C for experimental durations of 240 and 480 h, with H_2O contents of 9.76 and 9.92 wt% H_2O, respectively (nos. 26 and 27a, Table 3). At the same conditions, H_2O contents obtained from hydrous glasses as starting material (diffusion rates of H_2O are higher in hydrous glasses) are 9.80 and 9.97 wt% H_2O for experimental durations of 120 and 672 h, respectively (nos. 24 and 25, Table 3). For smaller samples (3 mm), used in most experiments, the H_2O contents were not systematically higher in experiments of long duration (see expts. 2, 3, 4 and 18, 19 in Table 3, HPG6–HPG12 at 1 kbar and 850 °C in Table 2). Thus, experimental durations of 10 d or more were sufficient to hydrate completely the dry starting glasses (cylinders of 3 mm length) used to determine the compositional dependence of H_2O solubility in this study. In addition, considering diffusion coefficients of H_2O of 4.5×10^{-8}–7.5×10^{-8} cm^2/s between 800 and 850 °C, respectively (Lapham et al., 1984; Zhang et al., 1991), it can be shown that these durations are sufficient for complete homogenization of the glass cylinders by diffusion of H_2O. Some experiments carried out at higher temperatures (1000–1350 °C) with composition AOQ or with hydrous starting glasses were shorter (Table 3), but H_2O diffusion was shown to be faster under those conditions (Lapham et al., 1984; Nowak and Behrens, 1992).

Loss of H_2O during and after quenching

The negative temperature dependence of H_2O solubility at $P \leq 4$ kbar implies that no H_2O should leave the melt during isobaric quenching. In contrast, at 5 kbar, H_2O solubility decreased with decreasing T (Fig. 4), and some dissolved H_2O may have exsolved from the melt during isobaric quenching. This probably explains the existence of small bubbles in some 5 kbar samples. Glass blocks (containing the bubbles) were used for KFT on these samples, and the H_2O content determined represents that of the melt at the experimental T.

The effect of the quench rate on measured values of H_2O solubility was tested at 5 kbar (expts. 27b and 27c, Table 3). In the first step, a glass was saturated with H_2O (no. 27a). One piece of this glass, containing 9.9 wt% H_2O, was placed in a CSPV for 16 h and quenched from 800 to 100 °C in 5 min; the other was quenched in 15 s. The small difference observed (0.1 wt% H_2O lower for the rapidly quenched sample) is probably insignificant.

Because of the high H_2O contents in some samples and especially in the 8-kbar samples, H_2O might have left the glass at room temperature. For the 5-kbar experiments, care was taken to open the capsules just before the determination of the H_2O content by KFT. The 8-kbar capsules were placed in ice just after quenching and were quickly analyzed for their H_2O content. For experiment no. 33 (Table 3), a second analysis performed 3 h later yielded a significantly lower H_2O content (13.32 wt% H_2O instead of 13.85).

TABLE 5. Compositions of anhydrous and hydrous glasses

No.	HPG6	HPG6	HPG6	HPG6	HPG6	HPG5	HPG9
H_2O (wt%)*	0	2.66	4.44	6.41	6.53	5.58	5.97
n	10	9	10	8	8	7	6
K_2O	0.91	0.87	0.85	0.84	0.83	8.25	5.52
Na_2O	6.85	6.68	6.48	6.14	6.29	2.26	3.29
Al_2O_3	12.80	12.36	12.04	11.86	11.81	12.89	11.25
SiO_2	78.41	76.48	74.86	73.24	73.56	70.07	72.94
Total	98.97	96.39	94.23	92.38	92.49	93.47	93.00
Composition recalculated to 100%							
K_2O	0.92	0.91	0.90	0.91	0.90	8.83	5.93
Na_2O	6.92	6.93	6.88	6.66	6.80	2.42	3.54
Al_2O_3	12.92	12.82	12.78	12.88	12.77	13.79	12.10
SiO_2	79.22	79.34	79.43	79.53	79.53	74.96	78.43

Note: microprobe analyses were performed at Orléans (BRGM-CNRS) with a Cameca SX50 (analytical conditions: 6 nA, 15 kV, 10-μm beam, 5-s counting time for Na and K, 10-s counting time for Si and Al). Analytical data are averages of n microprobe analyses.

* Determined from KFT.

Composition of the melt

The presence of a (H_2O-rich) fluid phase in equilibrium with the melt may have affected its composition, because of incongruent dissolution of the silicate melt in the fluid phase. However, in most experiments, the added amounts of H_2O were only slightly higher than the expected H_2O solubility. Due to the high ratio of melt to fluid, the composition of the melt is very little affected by dissolution of silicate in the fluid, as shown in Table 5. The composition of HPG6 glasses (microprobe analyses performed with Cameca SX50 at BRGM-CNRS, Orléans) does not show any significant variation of K, Na, Al, or Si contents as a function of the H_2O content of the melt (0–6.5 wt% H_2O). The small difference between the composition of the dry HPG6 glass given in Table 1 and that in Table 5 may result from the use of different analytical conditions and apparatus (microprobes in Bayreuth and Orléans for Tables 1 and 5, respectively). The compositions of HPG5 and HPG9 hydrous glasses (5.5 and 5.9

wt% H_2O, respectively) are very close to the composition of their dry equivalents given in Table 1.

Comparison with previous experimental data in the system Qz-Ab-Or

Temperature dependence. The temperature dependence of H_2O solubility observed in this study is in good agreement with that observed by Oxtoby and Hamilton (1979) and Hamilton and Oxtoby (1986) for Ab melts. At 2 kbar, Holtz et al. (1992a) recorded the same temperature dependence observed by Hamilton and Oxtoby (1986: a decrease in H_2O solubility of 0.15 ± 0.05 wt% H_2O for an increase in T of 100 °C). Oxtoby and Hamilton (1979) also noted that the temperature dependence of H_2O solubility changes from being negative at low P ($P < 4$ kbar) to slightly positive at high P ($P > 4$ kbar). At 4 kbar, they found no temperature dependence of H_2O solubility in Ab melts.

Pressure dependence. The pressure dependence of H_2O solubility for binary haplogranite compositions (Qz-Ab, Qz-Or) was investigated by Oxtoby and Hamilton (1978a, 1978b). The results are in good agreement at low P. However, at $P > 3$ kbar, our results show a significant almost linear dependence of H_2O solubility on P, whereas Oxtoby and Hamilton (1978a, 1978b) found only low variations with P (Fig. 5). This discrepancy may be due to the analytical method used by Oxtoby and Hamilton (drying at 105 °C), which may underrepresent the H_2O solubility determined at high H_2O contents. It has to be noted that Silver and Stolper (1989) concluded from calculations that the H_2O solubility determined at high pressure by Hamilton and Oxtoby (1986) is probably too low, which is in agreement with our experimental results.

Compositional dependence. There are few studies in which the compositional dependence of H_2O solubility in haplogranite melts has been investigated (Oxtoby and Hamilton, 1978a, 1978b, 1979, and Hamilton and Oxtoby, 1986, for Ab, Or, Qz-Ab, Qz-Or melts; Voigt et al., 1981, for Ab-Or melts; Dingwell et al., 1984, for Qz-Ab-Or melts). The higher H_2O solubility in Ab melts compared with Or melts has been observed previously (Oxtoby and Hamilton, 1978b; Voigt et al., 1981; see also review in McMillan and Holloway, 1987). Dingwell et al. (1984) suggested that there is no significant variation of H_2O solubility at 0.97 kbar between two ternary compositions with K/(Na + K) ratios of 0.428 and 0.309 and with approximately 35 wt% Qz. However, these compositions are not very different in terms of their alkali ratio, and the uncertainty given for the two compositions investigated by Dingwell et al. (1984) is within the variations observed in this study. On the basis of data from Tuttle and Bowen (1958), Luth (1976) estimated the H_2O solubility at 1 kbar for Qz-Ab, Qz-Or, Qz-Ab-Or eutectics and minimum compositions to be >4.8, 4.4, and 4.3 wt% H_2O, respectively. Slightly lower H_2O solubilities were found in this study (Fig. 2), but that may be due to the applied T (850 °C), which is higher than the eutectic or minimum temperatures. Thus, the values determined by Tuttle and Bowen (1958) are consistent with our 1-kbar data.

Comparison with calculations

Several methods have been used to calculate H_2O solubility curves, or more generally phase relations, for aluminosilicate systems (e.g., Spera, 1974; Burnham, 1979; Nicholls, 1980; Burnham and Nekvasil, 1986; Silver and Stolper, 1985, 1989; Blencoe, 1992). Spera (1974) and Blencoe (1992) used a binary solution model involving Margules type expansions. In the case of binary systems (for example Ab-H_2O), the Margules method was used successfully for thermodynamic modeling (Blencoe, 1992). However, the application of this method for multicomponent silicate systems (Spera, 1974) implies that empirical parameters have to be defined by least-squares analysis of the experimental H_2O solubility data. Until now, an accurate prediction of H_2O solubility for ternary (Qz-Ab-Or) compositions remained difficult because no systematic experimental data existed.

Burnham and Nekvasil (1986) extended the Ab-H_2O solution model (Burnham and Davis, 1974) and proposed the revised quasi-crystalline model of hydrous silicate melts to predict H_2O solubilities (and phase relations) in haplogranitic systems (Qz-Ab-Or-H_2O). The H_2O solubilities calculated at 900 °C using the model of Burnham and Nekvasil (1986) are given in Table 4 and can be compared with the experimentally determined H_2O solubilities (recalculated for 900 °C). At 1 and 2 kbar, the values are relatively close to those observed experimentally, especially for compositions close to the ternary minima (HPG8). Although only slightly different from the experimental data, the calculated H_2O solubilities are systematically higher at 0.5 kbar. They are significantly lower at 5 kbar (by 0.86–2.19 wt% H_2O, see Fig. 8). In terms of mole fractions, the calculated H_2O solubilities are constant for a given Qz content (because equimolal isothermal isobaric H_2O solubility is assumed in feldspar melts), which is not in agreement with the experimental results between 1 and 5 kbar (Fig. 8). Thus, H_2O solubilities calculated using the model of Burnham and Nekvasil (1986) underestimate the role of alkalis in melts (Na, K) at $P \geq 1$ kbar. This might have important petrological consequences for predicted phase relations in aluminosilicate-H_2O systems (i.e., Nekvasil and Burnham, 1987; Nekvasil, 1990) and for calculated H_2O activities (especially at 5 kbar). The alkali effect on the H_2O solubility observed in this study may also explain the difference between the experimentally determined H_2O-undersaturated liquidus phase relations in the system Qz-Ab-Or-H_2O-CO_2 (Ebadi and Johannes, 1991; Holtz et al., 1992b; Pichavant et al., 1992) and the calculated H_2O-undersaturated phase relations in the system Qz-Ab-Or-H_2O (Nekvasil and Burnham, 1987).

The thermodynamic model of Silver and Stolper (1985) allowing H_2O solubility to be calculated is based on ideal mixing of OH groups, molecular H_2O, and O atoms in the melt. Because the exact proportion of H_2O and OH

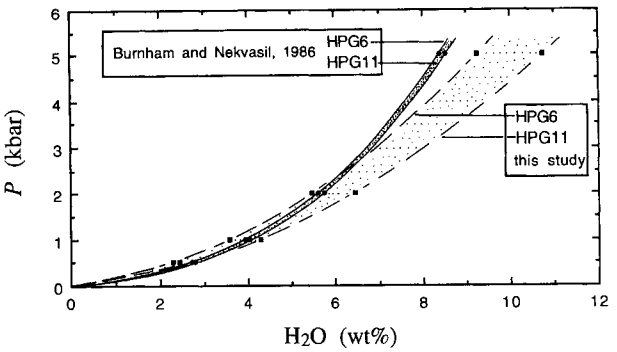

Fig. 8. Comparison of experimentally determined H_2O solubilities for melt compositions HPG6 and HPG11 with calculated H_2O solubilities after Burnham and Nekvasil (1986). The dotted areas represent the fields of H_2O solubility for compositions HPG6 to HPG11. Experimentally determined and calculated H_2O solubilities are given for 900 °C (data given in Table 4).

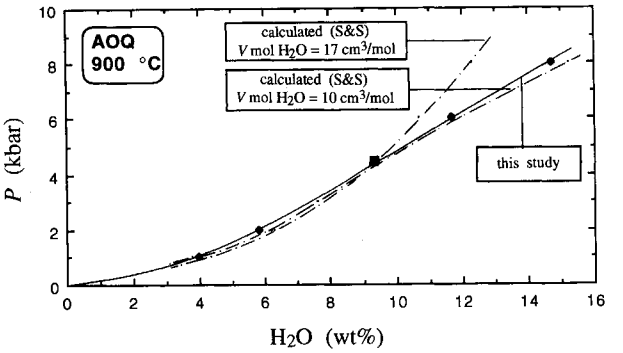

Fig. 9. Pressure dependence of H_2O solubility for composition AOQ at 900 °C calculated after the thermodynamic model of Silver and Stolper (1985) (S&S) and after the experimental data of this study. The continuous curve, diamonds and square are extrapolated from the experimental data (Tables 3 and 4). Broken curves (S&S) are calculated after Silver and Stolper (1985) for partial molar volumes of H_2O of 10 and 17 cm³/mol. K_1 was taken to be 0.2; the reference point (square) corresponds to the H_2O solubility at 4.5 kbar (9.3 wt% H_2O). For further explanation, see text.

units is still under debate (e.g., Dingwell and Webb, 1990a), a reference point and the partial molar volume of H_2O (V_{H_2O}) in the melt have to be known for the calculations (Silver and Stolper, 1985). At the reference point, the H_2O solubility at a given P is independent of T. From this study, the H_2O solubility at the reference point for composition AOQ is well constrained and corresponds to 9.3 wt% H_2O (solubility at approximately 4.5 kbar). However, V_{H_2O} is not known for the investigated compositions and can change from 0 to 22 cm³/mol in rhyolitic to albitic liquids (Silver et al., 1990). This variation affects significantly the H_2O solubility for composition AOQ calculated after the model of Silver and Stolper (1985): a calculated H_2O solubility at 6 kbar and 900 °C changes from 13.3 to 10.0 wt% H_2O if V_{H_2O} increases from 0 to 22 cm³/mol (the following values were used for the calculation: $K_1 = 0.2$, $X_{Br} = 0.157$, $K_{2r} = 0.095$; for an explanation see Silver and Stolper, 1985). With V_{H_2O} close to that estimated for albite melts at high pressure (17 cm³/mol), $K_1 = a^2_{OH}/(a_O \cdot a_{H_2O\ mol}) = 0.2$ (where a_{OH}, $a_{H_2O\ mol}$, and a_O refer to the activities of OH groups, molecular H_2O, and O atoms not associated with H atoms in the melt), and a H_2O solubility of 9.3 wt% H_2O at the reference point (4.5 kbar), the calculated and experimentally determined H_2O solubilities at 900 °C are in relatively good agreement at $P < 6$ kbar (Fig. 9), but there is a significant difference at 8 kbar (the calculated H_2O solubility at 900 °C is 12.3 wt% H_2O, whereas the value determined experimentally is higher than 13.8 wt% H_2O; see Table 3). At all pressures between 1 and 8 kbar, the best agreement between calculated and experimental values is obtained for a V_{H_2O} close to 10–12 cm³/mol (Fig. 9). However, it has to be noted that V_{H_2O} is not necessarily constant over this pressure range, and that this value of V_{H_2O} is only valid if K_1 is close to 0.2 and if ideal mixing of H_2O, OH and O units is assumed. Other models involving nonideal mixing of these units have also been developed by Silver and Stolper (1989). However, as outlined by the authors, the proportions of OH and H_2O units in melts have to be known, and consistent H_2O solubility data sets for binary compositions (such as Ab-H_2O, Or-H_2O, Qz-H_2O) have to be tested first in order to find out the model that can retrieve all measurements.

Implications

H_2O solubility mechanisms in aluminosilicate melts

The existence of different dissolved hydrous species in aluminosilicate melts has been proposed by several authors on the basis of experimental H_2O solubility data (Oxtoby and Hamilton, 1978a) and spectroscopic investigations of hydrous glasses (e.g., Stolper, 1982; Mysen and Virgo, 1986; Kohn et al., 1989; Silver and Stolper, 1989; Silver et al., 1990; Sykes et al., 1993).

The existence of at least two solubility mechanisms for H_2O between 0 and 5 kbar was suggested by Oxtoby and Hamilton (1978a) because of the existence of two trends when plotting H_2O solubility data as a function of the square root of f_{H_2O} (Fig. 10). The H_2O solubility value at the transition between the two mechanisms is approximately 6.5 wt% H_2O for Qz-Ab melt (with composition $Na_2O \cdot Al_2O_3 \cdot 10SiO_2$). If our solubility data, expressed in mole percent, are plotted against the square root of f_{H_2O}, the two distinct trends obtained by Oxtoby and Hamilton (1978a, 1978b) are not observed (Fig. 10) because of the larger H_2O solubility dependence on P (at $P \geq 3$ kbar) found in this study (see above and Fig. 5).

There is now an overall agreement that H_2O dissolved in aluminosilicate melts is present as both molecular H_2O and OH groups (e.g., Stolper, 1982; Silver and Stolper, 1989; Silver et al., 1990). On the basis of spectroscopic studies of quenched glasses, Silver and Stolper (1989) and

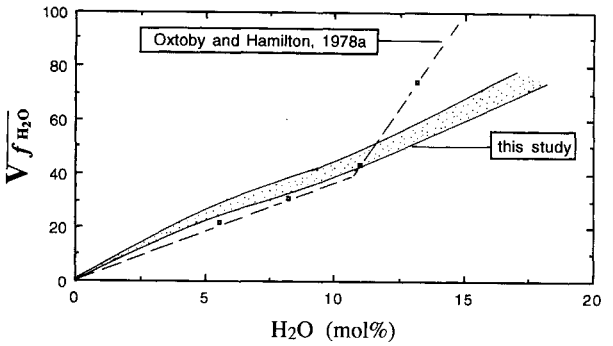

Fig. 10. H_2O solubility expressed as mole percent (on the basis of one O) plotted against the square root of f_{H_2O}. All H_2O solubility data (at 900 °C) determined in this study plot within the dotted area. The dashed straight lines represent the H_2O solubility curve determined by Oxtoby and Hamilton (1978a) for a Qz-Ab melt at 1000 °C. H_2O fugacity values are from Burnham et al. (1969).

Silver et al. (1990) have suggested that the maximum amount of H_2O incorporated as OH groups is 2.3 wt% H_2O in Ab melts and 2 wt% H_2O in Or melts, and that it is attained for a total H_2O content of approximately 4 wt% H_2O. At higher H_2O contents, all additional H_2O is incorporated as molecular H_2O according to this model, and in all our experiments with melts containing 4 wt% H_2O or more ($P \geq 1$ kbar) the OH contents should be at their maximum values. The difference in H_2O solubility due to OH groups between Qz- and Ab-rich and Qz- and Or-rich melts should be only 0.3 wt% H_2O. Thus, according to Silver and Stolper (1989) and Silver et al. (1990), the higher H_2O solubilities observed in the Ab-rich melts (Figs. 6 and 7) and the linear correlation between H_2O solubility and pressure between 3 and 8 kbar (Figs. 5 and 6) would be related to molecular H_2O in the melts. However, it has to be emphasized that the amount of OH groups analyzed by Silver and Stolper (1989) and Silver et al. (1990) from quenched glasses may be higher than 2 wt% H_2O because H_2O speciation is temperature dependent (Stolper, 1989) and, consequently, may be strongly quench-rate dependent (Dingwell and Webb, 1990a). The results of Stolper (1989) and the analysis by Dingwell and Webb (1989, 1990b) suggest that OH contents in aluminosilicate melts at hyperliquidus temperatures may be significantly higher than OH contents at the glass transition.

The alkali effect observed for the variation of H_2O solubilities between 1 and 5 kbar (H_2O solubility is the highest in the most Ab-rich melts, see Figs. 2, 3, and 7) can be explained by the incorporation mechanism of H_2O proposed by Pichavant et al. (1992), which suggests that the different amount of H_2O observed in haplogranite melts (with compositions close to those investigated in this study) can be due to the existence of hydrated $K(OH)(H_2O)_n$ and $Na(OH)(H_2O)_n$ clusters. Because of the larger size of K and of the longer K-O bond length when compared with Na-O (Brown et al., 1988), the n molecules of H_2O in $K(OH)H_2O_n$ clusters should be lower than those in $Na(OH)H_2O_n$ clusters at the same P-T conditions.

It is difficult to estimate if the alkali effect observed in melts containing high molecular H_2O contents also exists in melts with high proportions of OH ($P \leq 0.5$ kbar) because the observed differences between Ab-rich and Or-rich melts at 0.5 kbar are weak (H_2O solubility between 2.11 and 2.46 wt% H_2O at 1000 °C, Fig. 1). However, the maximum H_2O solubility systematically observed at 0.5 and 0.52 kbar for intermediate compositions with X_{Or} between 0.38 and 0.23 (see Table 2 and Fig. 7) suggests that the alkali effect observed at higher P is significantly lower at 0.5 kbar, if it exists at all.

It is difficult to predict the consequences of the results obtained in this study (Qz-Ab-Or compositions) for the Ab-Or system. That H_2O solubility in Ab melts is higher than in Or melts is known from previous studies. However, at high P (>3 kbar), the difference between the two compositions is probably higher than that determined by Oxtoby and Hamilton (1978a). The approximately linear evolution of H_2O solubility with changing Ab-Or content observed at 4.8 kbar in ternary compositions (Fig. 7) cannot be extrapolated to the Ab-Or join, because nonideal interactions occur between Na- and K-bearing structural units along this join, as shown by Voigt et al. (1981) at 5 kbar. This suggests that the incorporation mechanisms of H_2O may change significantly with changing silica content. The investigation of the effect of silica content along the Qz-Ab and Qz-Or joins is needed to determine to what extent the H_2O solubility mechanisms in Ab or Or melt, such as proposed by Kohn et al. (1989) or Sykes et al. (1993), can be extended to ternary compositions.

Petrological implications

The H_2O solubility data given in this study have important petrological implications for both physical and chemical properties of granitic melts. Combined with the results of Urbain et al. (1982), showing that dry $NaAlSi_3O_8$ liquids are less viscous than $KAlSi_3O_8$ liquids at fixed T, the higher H_2O solubility in Ab-rich melts demonstrated in this study implies that H_2O-saturated Ab-rich melts might be much less viscous than Or-rich melts. The compositional dependence of H_2O solubility also suggests that, for a given H_2O content of the melt, degassing by second boiling in an Ab-rich granitic melt may occur at a pressure lower than that in a Or-rich melt.

The compositional dependence of H_2O solubility in the system Qz-Ab-Or implies that H_2O-saturated phase relations, such as isobarical polythermal liquidus surfaces defined by Tuttle and Bowen (1958) and Luth et al. (1964), are not determined at a constant H_2O content of the melt (Pichavant, 1990). The liquidus temperatures change if a Qz-Ab-Or section is constructed at constant pressure and H_2O content of the melt (Fig. 11). Using the data of Holtz et al. (1992b) and Pichavant et al. (1992), obtained in the H_2O-saturated and H_2O-undersaturated Qz-Ab-Or system, a section along the cotectic curves separating the

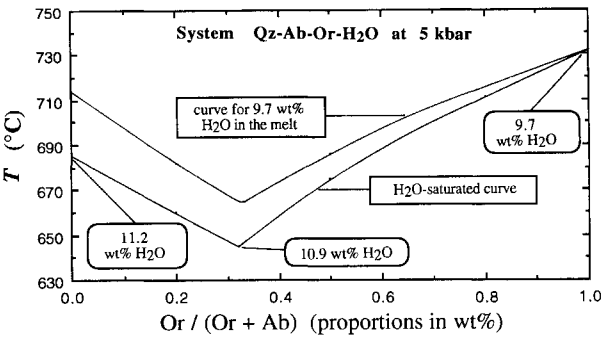

Fig. 11. Section along the cotectic curves separating the quartz and feldspar primary fields in the system Qz-Ab-Or-H_2O at 5 kbar. The quartz content of the eutectic or cotectic compositions varies approximately between Qz_{30} and Qz_{45}. Along the H_2O-saturated cotectic curve, the H_2O content of the melt increases progressively (see indicated H_2O solubility values) with increasing Ab content of the melt. The H_2O solubility in the Qz-Or eutectic melt at the liquidus temperature is 9.7 wt% H_2O. If a cotectic curve is recalculated for 9.7 wt% H_2O, the liquidus temperature increases by 28 °C at the Qz-Ab eutectic point and by 20 °C at the thermal minimum when compared with H_2O-saturated conditions. The cotectic curve for 9.7 wt% H_2O in the melt is calculated using H_2O-undersaturated phase relations given by Holtz et al. (1992b). H_2O solubilities are calculated from this study. (Source of data for H_2O-saturated cotectic curve: Holtz et al., 1992b.)

quartz and feldspar primary fields is shown for H_2O-saturated conditions and for a H_2O content of the melt of 9.7 wt% on Figure 11 (9.7 wt% H_2O is the calculated H_2O solubility for the Qz-Or eutectic at 5 kbar). Liquidus temperatures for Qz- and Ab-rich compositions containing 9.7 wt% H_2O are higher by 20–30 °C than the 5-kbar H_2O-saturated liquidus temperatures, whereas the liquidus temperature for the Qz-Or eutectic remains unchanged.

Acknowledgments

This work was supported by Procope (a German-French research program between Hanover and Orléans) DFG grant Di 431/3-1, and SFB 173 (German Sonderforschungsbereich). Technical assistance was provided by O. Diedrich, A. Lefèvre, M. Nowak, F. Schulze, H. Schulze, and D. Krauße. Helpful and constructive reviews by P. Ihinger and D. Joyce are particularly appreciated.

References cited

Blencoe, J.G. (1992) A two-parameter Margules method for modelling the thermodynamic mixing properties of albite-water melts. Transactions of the Royal Society of Edinburgh Earth Sciences, 83, 423–428.

Brown, G.E., Ponader, C.W., Waychunas, G.A., and Jackson, W.E. (1988) EXAFS studies of cation environment in silicate melts and glasses (abs.). European Association for Geochemistry, International Congress of Geochemistry and Cosmochemistry, Chemical Geology, 70, 86.

Burnham, C.W. (1979) The importance of volatile constituents. In H.S. Yoder, Ed., The evolution of the igneous rocks, fiftieth anniversary perspectives, p. 439–482. Princeton University Press, Princeton, New Jersey.

Burnham, C.W., and Davis, N.F. (1974) The role of H_2O in silicate melts: II. Thermodynamic and phase relations in the system $NaAlSi_3O_8$-H_2O to 10 kbar, 700° to 1100 °C. American Journal of Science, 274, 902–940.

Burnham, C.W., and Nekvasil, H. (1986) Equilibrium properties of granite pegmatite magmas. American Mineralogist, 71, 239–263.

Burnham, C.W., Holloway, J.R., and Davis, N.R. (1969) Thermodynamic properties of water to 1000 °C and 10,000 bars. Geological Society of America Special Paper, 132, 71–83.

Dingwell, D.B. (1987) Melt viscosities in the system $NaAlSi_3O_8$-H_2O-F_2O_{-1}. In B.O. Mysen, Ed., Magmatic processes: Physicochemical principles. Geochemical Society Special Publication, 1, 423–431.

Dingwell, D.B., and Webb, S.L. (1989) Structural relaxation in silicate melts and non-Newtonian melt rheology in igneous processes. Physics and Chemistry of Minerals, 16, 508–516.

——— (1990a) The temperature-dependence of water speciation in rhyolitic melts: Analysis of quenchrate-dependent speciation data using relaxation theory. Eos, 70, 501–502.

——— (1990b) Relaxation in silicate melts. European Journal of Mineralogy, 2, 427–449.

Dingwell, D.B., Harris, D.M., and Scarfe, C.M. (1984) The solubility of H_2O in melts in the system SiO_2-Al_2O_3-Na_2O-K_2O at 1 to 2 kbars. Journal of Geology, 92, 387–395.

Ebadi, A., and Johannes, W. (1991) Experimental investigation of composition and beginning of melting in the system $NaAlSi_3O_8$-$KAlSi_3O_8$-SiO_2-H_2O-CO_2. Contributions to Mineralogy and Petrology, 106, 286–295.

Hamilton, D.L., and Oxtoby, S. (1986) Solubility of water in albite melt determined by the weight-loss method. Journal of Geology, 94, 626–630.

Holtz, F., Behrens, H., Dingwell, D.B., and Taylor, R.P. (1992a) Water solubility in aluminosilicate melts of haplogranite composition at 2 kbar. Chemical Geology, 96, 289–302.

Holtz, F., Pichavant, M., Barbey, P., and Johannes, W. (1992b) Effects of H_2O on liquidus phase relations in the haplogranite system at 2 and 5 kbar. American Mineralogist, 77, 1223–1241.

Holtz, F., Dingwell, D.B., and Behrens, H. (1993) Effects of F, B_2O_3, P_2O_5 on the solubility of water in haplogranite melts compared to natural silicate melts. Contributions to Mineralogy and Petrology, 113, 492–501.

Kohn, S.C., Dupree, R., and Smith, M.E. (1989) A multinuclear magnetic resonance study of the structure of hydrous albite glasses. Geochimica et Cosmochimica Acta, 53, 2925–2935.

Lapham, K.E., Holloway, J.R., and Delaney, J.R. (1984) Diffusion of H_2O and D_2O in obsidian at elevated temperatures and pressures. Journal of Non-Crystalline Solids, 67, 179–191.

Luth, W.C. (1976) Granitic rocks. In D.K. Bailey and R. MacDonalds, Eds., The evolution of the crystalline rocks, p. 335–417. Academic Press, London.

Luth, W.C., Jahns, R.H., and Tuttle, O.F. (1964) The granite system at pressures of 4 to 10 kilobars. Journal of Geophysical Research, 69, 759–773.

McMillan, P.F., and Holloway, J.R. (1987) Water solubility in aluminosilicate melts. Contributions to Mineralogy and Petrology, 97, 320–332.

Mysen, B.O., and Virgo, D. (1986) Volatiles in silicate melts at high pressure and temperature: I. Interaction between OH groups and Si^{4+}, Al^{3+}, Ca^{2+}, and H^+. Chemical Geology, 57, 303–331.

Nekvasil, H. (1990) Reaction relations in the granite system: Implications for trachytic and syenitic magmas. American Mineralogist, 75, 560–571.

Nekvasil, H., and Burnham, C.W. (1987) The calculated individual effects of pressure and water content on phase equilibria in the granite system. In B.O. Mysen, Ed., Magmatic processes: Physicochemical principles. Geochemical Society Special Publication, 1, 433–445.

Nicholls, J. (1980) A simple thermodynamic model for estimating the solubility of H_2O in magmas. Contributions to Mineralogy and Petrology, 74, 211–220.

Nowak, M., and Behrens, H. (1992) Water diffusion in albitic and haplogranitic melts. Terra Abstracts, 1, 31–32.

Oxtoby, S., and Hamilton, D.L. (1978a) The discrete association of water with Na_2O and SiO_2 in NaAl silicate melts. Contributions to Mineralogy and Petrology, 66, 185–188.

——— (1978b) Calculation of the solubility of water in granitic melts. In W.S. McKenzie, Ed., Progress in experimental petrology. Natural Environmental Research Council Publications Series D, no. 11, p. 37–40. Department of Geology, Manchester University, Manchester, U.K.

——— (1979) The solubility of water in alkali-aluminosilicate melts to 8 kbars. In K.D. Timmerhaus and M.S. Barber, Eds., High-pressure science and technology. Sixth AIRAPT conference, p. 153–158. Plenum, New York.

Pichavant, M. (1983) Melt-fluid interaction deduced from studies of silicate-B_2O_3-H_2O systems at 1 kbar. Bulletin de Minéralogie, 106, 201–211.

——— (1990) Phase equilibria in granitic systems: Implications for H_2O speciation in aluminosilicate melts (abs.). Terra Cognita, 2, 28.

Pichavant, M., Holtz, F., and McMillan, P. (1992) Phase relations and compositional dependence of H_2O solubility in quartz-feldspar melts. Chemical Geology, 96, 303–319.

Puziewicz, J., and Johannes, W. (1988) Phase equilibria and compositions of Fe-Mg-Al minerals and melts in water-saturated peraluminous granitic systems. Contributions to Mineralogy and Petrology, 100, 156–168.

Roux, J., and Lefèvre, A. (1992) A fast-quench device for internally heated pressure vessels. European Journal of Mineralogy, 4, 279–281.

Roux, J., Holtz, F., Lefèvre, A., and Schulze, F. (1994) A reliable high-temperature setup for internally heated pressure vessels: Applications to silicate melt studies. American Mineralogist, 79, 1145–1149.

Silver, L.A., and Stolper, E.M. (1985) A thermodynamic model for hydrous silicate melts. Journal of Geology, 93, 161–178.

——— (1989) Water in albitic glasses. Journal of Petrology, 30, 667–710.

Silver, L.A., Ihinger, P.D., and Stolper, E.M. (1990) The influence of bulk composition on the speciation of water in silicate glasses. Contributions to Mineralogy and Petrology, 104, 142–162.

Sorapure, R., and Hamilton, D.L. (1984) The solubility of water in melts of albite composition with varying additions of fluorine. In C.M.B. Henderson, Ed., NERC, Progress in experimental petrology, 6, 28–29.

Spera, F.J. (1974) A thermodynamic basis for predicting water solubilities in silicate melts and implications for the low velocity zone. Contributions to Mineralogy and Petrology, 45, 175–186.

Stolper, E.M. (1982) Water in silicate glasses: An infrared spectroscopic study. Contributions to Mineralogy and Petrology, 81, 1–17.

——— (1989) Temperature dependence of the speciation of water in rhyolitic melts and glasses. American Mineralogist, 74, 1247–1257.

Sykes, D., Sato, R., Luth, R.W., McMillan, P., and Poe, B. (1993) Water solubility mechanisms in $KAlSi_3O_8$ melts at high pressure. Geochimica et Cosmochimica Acta, 57, 3575–3584.

Turek, A., Riddle, C., Cozens, B.J., and Tetley, N.W. (1976) Determination of chemical water in rock analysis by Karl-Fischer titration. Chemical Geology, 17, 261–267.

Tuttle, O.F., and Bowen, N.L. (1958) Origin of granite in the light of experimental studies in the system $NaAlSi_3O_8$-$KAlSi_3O_8$-SiO_2-H_2O. Geological Society of America Memoir, 74, 145 p.

Urbain, G., Bottinga, Y., and Richet, P. (1982) Viscosity of liquid silica, silicates and aluminosilicates. Geochimica et Cosmochimica Acta, 46, 1061–1072.

Voigt, D.E., Bodnar, R.J., and Blencoe, J.G. (1981) Water solubility in melts of alkali feldspar composition at 5 kbar, 950°C. Eos, 62, 428.

Westrich, H.R. (1987) Determination of water in volcanic glasses by Karl-Fischer titration. Chemical Geology, 63, 335–340.

Zhang, Y., Stolper, E.D., and Wasserburg, G.J. (1991) Diffusion of water in rhyolitic glasses. Geochimica et Cosmochimica Acta, 55, 441–456.

Manuscript received January 11, 1994
Manuscript accepted September 3, 1994